Fluid–Structure Interaction Simulation: Effect of Endovascular Coiling in Cerebral Aneurysms Considering Anisotropically Deformable Walls

Vidhya Vijayakumar and J. S. Jayakumar

Abstract In the present research, we use fluid–structure interaction to study the effect of endovascular coiling in brain aneurysms. We simulate pulsatile flow of blood through a tubular hypothetical bulge filled with a homogenous porous medium; however, the wall mechanical properties of the aneurysm wall are different from that of the non-aneurysmal vascular vessel wall. The numerical simulations were carried out using Open FOAM. The FSI technique has a nonlinear material model to represent the ICA tissue. Fully implicit method of coupling employed ensured that the solid and the fluid domain attained convergence at each of the time steps. The results from the FSI simulations show that the presence of a coil in an aneurysm sac reduces fluid loading within the sac, and hence, the velocity of blood flow becomes negligible within the aneurysm. The von Mises stresses and the wall shear stress values on the wall of the aneurysm decrease to a great extent after the coil is inserted. Consequently, the displacement of the blood vessel's wall also decreases, and hence, the risk of rupture of the aneurysm reduces. In conclusion, treatment using endovascular coiling technique delays further disintegration of the blood vessel and hence proves to be an effective treatment technique for cerebral aneurysm.

Keywords Cerebral aneurysm · Endovascular coiling · Fully implicit coupling · ICA tissue · Fluid–structure interaction

V. Vijayakumar (✉) · J. S. Jayakumar
Department of Mechanical Engineering, Amrita Vishwa Vidyapeetham, Amritapuri, India
e-mail: vidhya94vijay@gmail.com

J. S. Jayakumar
e-mail: jsjayan@gmail.com

P. Saha et al. (eds.), *Advances in Fluid and Thermal Engineering*,
Lecture Notes in Mechanical Engineering,
https://doi.org/10.1007/978-981-13-6416-7_41

1 Introduction

An intracranial aneurysm, generally occurring at the base of the brain, is a condition when a local and progressive balloon-like dilation occurs in the arteries. The initiation, growth, and the rupture of an aneurysm are generally associated with hemodynamic factors including wall shear stress, wall pressure, and flow rate of blood [1]. The commonly employed treatment options for a cerebral aneurysm include endovascular coiling and surgical clipping. In endovascular coiling embolization, a coil is inserted into the aneurysm sac, which averts blood circulation in the aneurysm, and ultimately, further rupture of the aneurysm can be prevented while in case of surgical clipping blood flow to the aneurysm is averted by placing a clip at the aneurysm neck.

The effect of stents on intra-aneurysmal flow using an ideal geometry has been experimentally investigated by Canton et al. [2]. Majority of the aneurysms generally occur at the bifurcation point of the blood vessel. This can be attributed to the fact that the risk of rupture associated with these sites increases manifolds due to the high magnitude of the wall shear stress. Flow shear stress may result in the dysfunction of endothelial cells, which leads to the destruction of the vessel walls [3]. Mitsos et al. [4] have investigated the effect of endovascular treatment on a patient-specific geometry.

The numerical simulation of the blood flow can effectively predict growth and rupture of aneurysm with minimal cost [5]. The study of the interaction of blood flow and the vessel walls is essential to predict this, owing to the elastic nature of the vessel. Hence, the fluid–structure interaction (FSI) simulation method is implemented in the current work.

The use of FSI simulations to determine the stress distribution within the wall of a hypothetical ICA geometry prior to treatment as well as after treatment using coil embolization technique, considering inconsistent mechanical properties for the aneurysm wall as well as that of the unaffected vessel wall, is described in this article. The FSI technique was implemented using OpenFOAM. The aim of this work was to study the effect of endovascular coiling in the prevention of further disintegration of an aneurysm wall.

2 Mathematical Modeling

2.1 Geometry

The fluid geometry under consideration is a bent tube with a sphere-shaped aneurysm as shown in Fig. 1 [6].The dimensions of the geometry have been scaled up by a factor of 4 in comparison to a human subject [7]. The aneurysms of this model have been found in patients [8]. Dynamic similarity has been ensured by maintaining the same values of the Reynolds number and Womersley number (*Re*

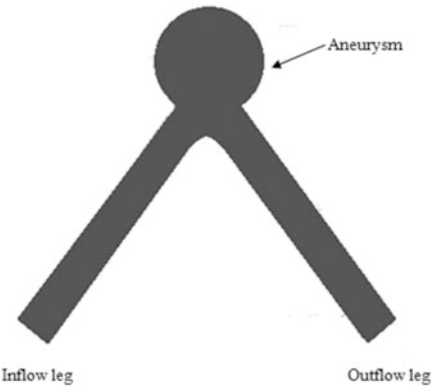

Fig. 1 Geometrical model for aneurysm analysis

and *Wo*). The diameter of the tube (*d*) is 10 mm. The length of the legs is considered 70 mm so that fully developed flow enters the aneurysm. The angle between the two legs of the tube is 75 °C. The bulge parameter is $D/d = 3$, for the model given below.

For the solid domain, different wall thickness was considered for the tube region and the bulge region. The tube wall thickness, excluding the bulge region, was considered to be 0.3 mm [9]. The minimum thickness of an aneurysm before rupture was reported to be 0.05 mm by Abruzzo et al. [10]. So, the thickness of 0.20 mm was used for the bulge. In the second case, the aneurysm was considered to be fully filled with a porous medium to model endovascular coiling treatment in cerebral aneurysm.

2.2 Governing Equations and Boundary Conditions

Fluid region. The blood flow is laminar and pulsatile. Blood is modeled as an incompressible fluid with a density equal to 1050 kg/m^3. The porous medium is present in the bulge region.

The governing equations for incompressible fluid flow through the non-porous and porous media, Nield and Bejan [11]:

$$\frac{\partial u_i}{\partial x_j} = 0 \tag{1}$$

$$\frac{\partial u_i}{\partial t} + u_j \frac{\partial u_i}{\partial x_j} = -\frac{\partial p}{\partial x_i} + \frac{1}{Re}\frac{\partial}{\partial x_j}\left(\frac{\mu}{\mu_\infty}\left[\frac{\partial u_i}{\partial x_j}\frac{\partial u_j}{\partial x_i}\right]\right) - \frac{\phi}{ReDa}\frac{\mu_\infty}{\mu}u_i - \frac{C_f}{\sqrt{Da}}|u_i|u_i \tag{2}$$

The last three terms of Eq. (2) are referred to as the Brinkman, Darcy, and Forchheimer terms, respectively. For simulating flow through a clear medium,

Table 1 Parameters for governing equations

μ_o, $P_{a\text{-}s}$	μ_∞, $P_{a\text{-}s}$	M	n	a	ρ, kg/m^3	φ [20]	K, m^2 [20]	Cf [20]
0.16	0.0035	8.2	0.64	1.23	1050	0.735	1.55e−8	0.2

Darcy and Forchheimer terms will be zero. The non-Newtonian properties of blood are simulated using the Carreau–Yasuda model [12]:

$$\mu(\gamma) = \mu_\infty + \frac{\mu_0 - \mu_\infty}{(1 + m\gamma^n)^a} \tag{3}$$

where $\gamma = \left(0.5 e_{ij} e_{ij}\right)^{0.5}$ and, $e_{ij} = \frac{1}{2}\left(\frac{\partial u_i}{\partial x_j} + \frac{\partial u_j}{\partial x_i}\right)$

The term m represents the relaxation time, and terms μ_∞ and μ_o represent the viscosity at infinite and zero shear rate, respectively. The values are given in Table 1.

where φ = porosity, K = permeability and Cf = inertia coefficient for the porous media within the bulge. The Darcy number (Da) of the coil is $K/D^2 = 1.55 \times 10^{-4}$. For a Reynolds number of 480 and a frequency of $f = 1.2$ Hz, the Womersley number Wo was found to be 7.8 and is consistent with flow in the brain.

$$Wo = \frac{d}{2}\sqrt{\frac{2\pi f \rho}{\mu_\infty}} \tag{4}$$

For the unsteady flow simulation, at each time step the Womersley profile [13] as given in Fig. 2 is specified as the inlet. Based on the inlet velocity profile, the mean Reynolds number was found to be 480. Pressure is specified as gradient outflow at the exit and has been derived from the work of Abdi et al. [14].

Solid Region. To the inner vascular wall of the geometry, 16 kPa (120 mm Hg) of peak systolic pressure was applied while zero external pressure was applied to

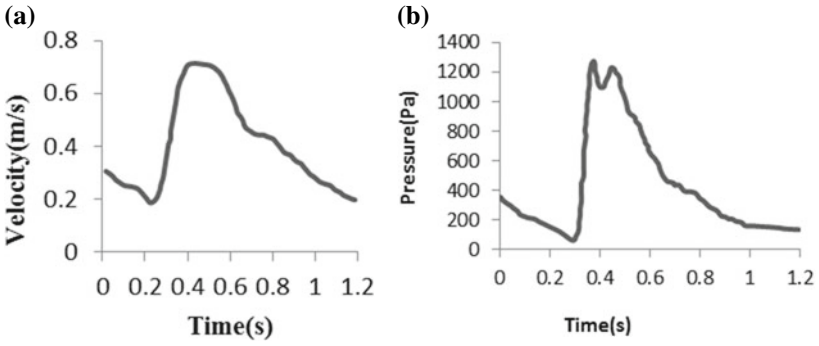

Fig. 2 **a** Inlet velocity boundary condition. **b** Outlet pressure boundary condition

the outer vascular wall. The mechanical properties assigned to the aneurysm and the arterial wall were different. A nonlinear elastic material is modeled as described by Kelly and O'Rourke [15], wherein the following procedure was used for simulating the solid domain. Based on the relationship between stress T and stretch ratio λ for the arterial wall, provided by Raghavan and Vorp [16]

$$T_1 = \left[2\alpha + 4\beta\left(\lambda_1^2 + 2\lambda_1^{-1} - 3\right)\right]\left[\lambda_1^2 - \lambda_2^{-1}\right] \tag{5}$$

Value of α and β was taken as 174000 and 1881000 Pa, respectively. Utilizing the previous relation an average stress–strain curve was calculated and is given by

$$\sigma = 2.744 \times 10^8 e^{7.275} - 2.744 \times 10^8 e^{7.272} \tag{6}$$

where ε represents strain and σ represents stress. The Young modulus of elasticity, E, is given by

$$E = \frac{\mathrm{d}\sigma}{\mathrm{d}\varepsilon} = 1996260000e^{7.275\varepsilon} - 1995436800e^{7.272\varepsilon} \tag{7}$$

The Young modulus of elasticity was then determined at each time step using the above equation. The material is now assumed to follow a linear elastic trend, and the corresponding values of displacement, stress, and strain are calculated. Similarly, the aneurysm was also modeled on the basis of the characteristics of intraluminal thrombus (ILT) as observed by Wang et al. [17].

$$T_1 = 2\left[c_1 + 2c_2\left(2\lambda_1 + \frac{1}{\lambda_1^2} - 3\right)\right] \tag{8}$$

The values of c_1 are taken as 28,000 Pa and c_2 as 28,600 Pa, respectively. The stress–strain relationship of ILT was calculated to be:

$$\sigma = 2.298 \times 10^7 e^{1.014\in} - 2.298 \times 10^7 e^{1.008\in} \tag{9}$$

Furthermore, the equation was differentiated to obtain a relationship for the Young modulus of elasticity, E

$$E = \frac{\mathrm{d}y}{\mathrm{d}x} = 23301720\mathrm{e}^{1.041\in} - 23163840\mathrm{e}^{1.008\in} \tag{10}$$

The momentum equation for a linear elastic material for the displacement d is given by

$$\frac{\partial^2(\rho d)}{\partial t^2} = \nabla.\left[\mu\nabla d + \mu(\nabla d)^{\mathrm{T}} + \lambda Itr(\nabla d)\right] \tag{11}$$

where μ and λ are Lame's coefficient which is related to Poisson's ratio v and Young's modulus of elasticity E as:

$$\mu = \frac{E}{2(1+\vartheta)} \text{ and } \lambda = \frac{\vartheta E}{(1+\vartheta)(1-2\vartheta)} \tag{12}$$

FSI Simulation. Iterations are separately carried out for both the fluid and solid systems to achieve convergence separately, and then, the entire system is solved for each time step, and hence, convergence is ensured. This is the general basis of various fluid–solid coupling codes which have been developed [18, 19].

2.3 Discretisation

The geometry was meshed in Gambit and thereafter imported into OpenFOAM. Mesh independency study was carried out considering both fluid and solid domains. The mesh independency studies produce the same results for 1.08 × 106 and 1.25 × 106 elements for the fluid region. For the solid domain, the value of maximum von Mises stress was used in order to conduct the mesh independency test and it was found that a mesh giving 1.21 × 105 elements, produced mesh-independent results. A grid quality of 0.9 was ensured throughout the geometry. The FSI solver was validated with the results of Kelly [15].

3 Results and Discussion

The quantities of interest in this study include (i) flow distribution, (ii) wall shear stress, (iii) wall pressure, (iv) von Mises stresses, and (v) wall displacement in the bulge.

3.1 Velocity Contour

In Fig. 3a, b, the time-averaged velocity contour has been shown in *x*-*y* mid-plane for the case prior to and succeeding endovascular treatment. The flow in the bulge is stronger in a clear media, and the corresponding velocities are subsequently greater in the case of clear medium. However, after the placement of a coil the circulating velocities in the bulge reduce. This is because of the fact that the coil is creating a bypass, which leads to a drastic reduction of the wall loading in the aneurysm.

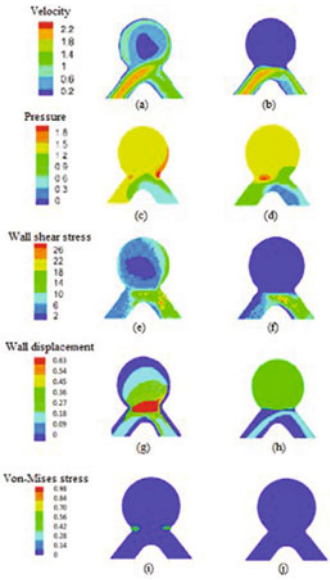

Fig. 3 Time-averaged contours of (**a**, **b**) absolute velocity (at mid-plane in front view), (**c**, **d**) wall pressure, (**e**, **f**) wall shear stress, (**g**, **h**) wall displacement (systolic phase) and (**i**, **j**) maximum von-Mises stress in clear media (first column) versus porous media (second column) for Re = 480 and Wo = 7.82

3.2 Pressure

The pressure levels were found to be marginally higher in the case of flow through a clear medium; however, from Fig. 3c, d it can be observed that pressure remains relatively unaffected by coil embolisation. This is because the bulge is a zone of separation even prior to the insertion of the coil, and hence, even after coil embolisation a uniform pressure exists because of low value of flow occurring within the bulge.

3.3 Wall Shear Stress

Time-averaged WSS contours are given for both the cases in Fig. 3e, f. The wall shear stress values were found to reduce nearly by a factor of 7 after insertion of coil, because of subsequent reduction of flow in the bulge. This can subsequently reduce the probability of rupture of the aneurysm.

3.4 Wall Displacement

Figure 3g, h shows the contour of solid displacement for both cases during the systolic phase. The maximum displacement is found to be 0.63 and 0.33 mm for the

case before and after coil embolisation, respectively. The value indicates that the maximum displacement for the treated aneurysm is 47% less than in case of untreated aneurysm. This clearly signifies that treatment using endovascular coiling can decrease the displacement of the blood vessel's wall and hence reduce the risk of rupture, thus proving to be an efficient treatment technique.

3.5 Von Mises Stress

Von Mises stress is a combination of the normal and shear stresses exerted on the solid wall. Hence, when compared to the material strength of the blood vessel's wall can determine the chances of rupture of the aneurysm wall. The contours of the von Mises stress that occur at the neck of the aneurysm have been given in Fig. 3i, j. The maximum stress for the cases prior to and succeeding treatment is 0.98 and 0.12 MPa, respectively. With the insertion of the coil, the relative reduction of the maximum von Mises stress is 87%.

4 Conclusion

In the present study, coil embolization modeling of cerebral aneurysm is reported. The coils are modeled as a porous medium. The linear elastic model is used to model the solid wall. The Womersley velocity profile is applied at the inlet of the fluid. The finite volume method is used to solve the unsteady state governing equations in 3D for both the solid and fluid solver. The results obtained show that in the presence of a coil in the bulge, the flow is bypassed, and the wall loading in the bulge drastically reduces. The wall shear stress decreases, and the displacement of the aneurysm wall is also found to decrease to a considerable extent. The von Mises stresses drastically reduce after coil embolization. However, the pressure was found to remain relatively unaffected. The percentage reduction in von Mises stress and the wall displacement was also appreciable. Thus, it is safe to conclude that coil embolization technique can be used to effectively treat cerebral aneurysms. Also, it can be concluded that FSI-based simulations can be effectively carried out to model blood flow in suitable biological models to determine the effectiveness of various treatment techniques. This solver can be applied to patient-specific models to effectively predict the response of the patient to the treatment.

References

1. Lieber BB et al (2002) Particle image velocimetry assessment of stent design influence on intra-aneurysmal flow. Annals of Biomed Eng 30(6):768–777

2. Cantón Gádor, Levy David I, Lasheras Juan C (2005) Changes in the intraaneurysmal pressure due to HydroCoil embolization. Am J Neuroradiol 26(4):904–907
3. Boussel L et al (2008) Aneurysm growth occurs at region of low wall shear stress: patient-specific correlation of hemodynamics and growth in a longitudinal study. Stroke 39 (11):2997–3002
4. Mitsos AP et al (2008) Haemodynamic simulation of aneurysm coiling in an anatomically accurate computational fluid dynamics model. Neuroradiology 50(4):341–347
5. Wu Jiacheng, Shadden Shawn C (2015) Coupled simulation of hemodynamics and vascular growth and remodeling in a subject-specific geometry. Ann Biomed Eng 43(7):1543–1554
6. Agrawal V et al (2015) Effect of coil embolization on blood flow through a saccular cerebral aneurysm. Sadhana 40(3):875–887
7. Weir B (1987) Aneurysms affecting the nervous system. Williams & Wilkins, Philadelphia
8. Gobin YP, Counord JL, Flaud P, Duffaux J (1994) In vitro study of haemodynamics in a giant saccular aneurysm model: influence of flow dynamics in the parent vessel and effects of coil embolisation. Neuroradiology 36(7):530–536
9. Torii R et al (2010) Influence of wall thickness on fluid–structure interaction computations of cerebral aneurysms. Int J Numer Methods in Biomed Eng 26(3–4):336–347
10. Abruzzo T et al (1998) Histologic and morphologic comparison of experimental aneurysms with human intracranial aneurysms. Am J Neuroradiol 19(7):1309–1314
11. Nield DA, Bejan A and Nield-Bejan (2006) Convection in porous media Vol. 3. Springer, New York
12. Leuprecht, A, Perktold, K (2001) Computer simulation of non-Newtonian effects of blood flow in large arteries. Comput Methods Biomech Biomed Eng 4:149–163
13. Hale JF, McDonald DA, Womersley JR (1955) Velocity profiles of oscillating arterial flow, with some calculations of viscous drag and the Reynolds number. J Physiol 128(3):629–640
14. Abdi M, Navidbakhsh M, Razmkon A (2016) A lumped parameter method to calculate the effect of internal carotid artery occlusion on anterior cerebral artery pressure waveform. J Biomed Phys Eng 6(1):33
15. Kelly SC, O'rourke MJ (2010) A two-system, single-analysis, fluid—structure interaction technique for modelling abdominal aortic aneurysms. Pro Inst Mech Eng, part H: J Eng Med 224(8):955–969
16. Raghavan ML, David A (2000) Vorp: toward a biomechanical tool to evaluate rupture potential of abdominal aortic aneurysm: identification of a finite strain constitutive model and evaluation of its applicability. J Biomech 33(4):475–482
17. Wang DHJ et al (2001) Mechanical properties and microstructure of intraluminal thrombus from abdominal aortic aneurysm. J Biomech Eng 123(6):536–539
18. Ivankovic A et al (2002) Towards early diagnosis of atherosclerosis: the finite volume method for fluid–structure interaction. Biorheol 39(3–4):401–407
19. Karac A, Ivankovic A (2003) Modelling the drop impact behaviour of fluid-filled polyethylene containers. In: European structural integrity society, Elsevier, Amsterdam, vol 32, pp 253–264, 2003
20. Kakalis NMP et al (2008) The haemodynamics of endovascular aneurysm treatment: a computational modelling approach for estimating the influence of multiple coil deployment. IEEE Trans Med Imaging 27(6):814–824